ELSEVIER

Specific heat measurements of TiB$_2$ and ^{6}LiF from 0.5 to 30 K

Brian E. Lang [a], Marcus H. Donaldson [a], Brian F. Woodfield [a,*], Arnold Burger [b], Utupal N. Roy [b], Vincent Lamberti [c], Zane W. Bell [d]

[a] *Department of Chemistry and Biochemistry, Brigham Young University, C100 Benson Science Building, P.O. Box 25700, Provo, UT 84602, United States*
[b] *Department of Physics, Fisk University, Nashville, TN 37208, United States*
[c] *Y-12 National Security Complex, P.O. Box 2009, Oak Ridge, TN 37831, United States*
[d] *Oak Ridge National Laboratory, Oak Ridge, TN 37831, United States*

Abstract

The specific heats of TiB$_2$ and ^{6}LiF have been measured from 0.5 to 30 K as part of a larger project in the construction of a neutron spectrometer. For this application, the measured specific heats were used to extrapolate the specific heats down to 0.1 K with lattice, electronic, and Schottky equations for the respective samples. The resultant specific heat values at 0.1 K for TiB$_2$ and ^{6}LiF are $4.08 \times 10^{-4} \pm 0.27 \times 10^{-4}$ J/K/mol and $9.19 \times 10^{-9} \pm 0.15 \times 10^{-9}$ J/K/mol, respectively.
© 2005 Elsevier B.V. All rights reserved.

1. Introduction

The genesis of this research is for the identification and development of materials suitable for use as absorbers in high-resolution cryogenic neutron spectrometers. It is well known that neutrons are difficult to detect since they are uncharged, thus their interaction with detectors is only via nuclear interactions. In addition, many of the older methods of neutron detection (such as the BF$_3$ detectors) were notorious for giving false signals from external heat sources if great care was not taken in the experimental design [1]. (This was the case for several researchers in the cold fusion debacle from 1989 to 1990 [1].) However, the aim of this project is to not only find a novel method to detect neutrons but to determine the energies of the incident neutrons as well.

The instrument design is a variation of a cryogenic gamma-ray spectrometer developed by Chow et al. [2] and employs a microcalorimeter comprised of an absorber, a thermometer, and weak thermal link to a cold bath to detect heat pulses associated with (n, α) reactions, details of which can be found elsewhere [3]. The thermometer in the current design is a superconducting transition edge sensor (TES) – a multilayer structure composed of alternating superconducting and non-superconducting films, which can enter the superconducting state at a temperature determined by the composition and

---

* Corresponding author. Tel.: +1 801 422 2093; fax: +1 801 422 0153.
E-mail address: brian_woodfield@byu.edu (B.F. Woodfield).

thickness of the layers. The TES is held in equilibrium near the low-temperature limit of the narrow transition between the superconducting (S) and normal (N) states, so that a small increase in temperature resulting from a single (n, α) reaction causes a large change in resistance from which the incident neutron energy is deduced.

The energy resolution of a detector of this type is determined by thermal fluctuations and Johnson noise and is given by
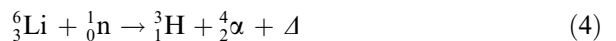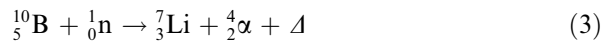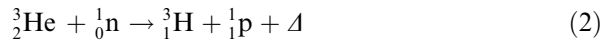
$$\Delta E = 2.35 \xi \sqrt{k_b T_{op}^2 C}, \tag{1}$$

where k_b is Boltzmann's constant, T_{op} is the operating temperature (Kelvin), C is the total heat capacity of the microcalorimeter, and ξ is a parameter dependent on the sensitivity of the thermometer and operating conditions [2,4]. Small values for ΔE (or higher energy resolution) can be obtained using small values of T_{op} and C. Chow et al. typically worked near 100 mK using a microcalorimeter with a total heat capacity of approximately 12.8×10^{-12} J/K (80 keV/mK) and a superconducting Sn absorber. The resulting resolution of the detector was 230 eV for 60 keV gamma rays [2].

In general, high-resolution neutron spectroscopy requires that the energy of an incident neutron be completely transformed to heat within the absorber so the signal will be proportional only to the sum of the kinetic energy of the neutron and the Q-value of the reaction. Practically, this means the neutron must take part in a nuclear reaction in the absorber in which few gamma rays and no neutrons are emitted, and the reaction products have short ranges. The constraint on gamma rays reflects the inability of a small detector volume to capture energy diverted to (n, γ) reactions. In addition, the absence of gamma-rays simplifies the response function. Neutron scattering reactions produce recoil ions with energies dependent on the incident neutron's energy, the angle through which it is scattered, the mass of the target atom, and the Q-value of the reaction. Since the scattered neutron may neither be captured nor sensed, its information can be lost, and this prevents accurate recovery of the incident energy.

Taking all of this into consideration, the ideal reactions for this type of neutron spectroscopy are those resulting in charged particles (protons, alpha particles, etc.). It is also desirable that the reaction products have sufficiently simple structures so their production in excited states is either forbidden by

conservation of energy or occurs with only a few Q-values. While fission reactions with actinides are seemingly excellent candidates, they must be rejected for this type of application since a significant amount of energy is lost to neutrons and gamma rays, and the fission products are complex enough to yield a wide range of Q-values. Instead, simple reactions involving ^{3}He, ^{10}B, and ^{6}Li are the most promising:

$$^3_2\text{He} + ^1_0\text{n} \rightarrow ^3_1\text{H} + ^1_1\text{p} + \Delta \tag{2}$$

$$^{10}_5\text{B} + ^1_0\text{n} \rightarrow ^7_3\text{Li} + ^4_2\alpha + \Delta \tag{3}$$

$$^6_3\text{Li} + ^1_0\text{n} \rightarrow ^3_1\text{H} + ^4_2\alpha + \Delta \tag{4}$$

where Δ represents the sum of the Q-value of the reaction (shared by the products) and the energy of the incident neutron, E_n. In most solids, the reaction products have ranges of a few microns if the incident neutrons have energies below 10 MeV.

Of these candidate nuclei, helium must be discarded immediately since it forms no known compounds and the Q-value for the (n, p) reaction is only 764 keV. With a Q-value this low, and a mass of only 3 amu, a ^{3}He nucleus recoiling from an (n, n) interaction with $E_n = 1$ MeV has roughly the same energy as the products resulting from a thermal neutron capture, which leads to a significant overlap of the capture and scattering signals and results in an indecipherable spectrum. On the other hand, the masses of lithium and boron, and the Q-values of the few accessible capture reactions, do allow the separation of capture events from scattering events based on pulse height. The ^{6}Li(n, α)t reaction produces an alpha particle and a triton (tritium nucleus) sharing $\Delta = 4.78$ MeV $+ E_n$. The ^{10}B$(n, \alpha)^7$Li reaction has two branches, with 94% of the reactions (at least at thermal energies) leaving ^{7}Li in its first excited state (0.478 MeV), and 6% leaving ^{7}Li in its ground state. The Q-values for these reactions are 2.310 and 2.792 MeV, respectively. Therefore, the initial search for the candidate material for the detector began with compounds of ^{6}Li and ^{10}B.

For the current design of the neutron spectrometer, Ti^{10}B$_2$ (30% ^{10}B, natural abundance) and ^{6}LiF (96% ^{6}Li) appear to fulfill all of the requirements. The neutron spectrometer is designed to operate at 0.1 K, and it is necessary to know the specific heat of the detector crystal at the operating temperature. However, previous measurements of the low-temperature specific heats of these samples have been inconsistent (especially with regards to TiB$_2$), so it is essential that the specific heat of materials be known

quite accurately at the detector operating temperatures. To this end, we have measured the specific heats of TiB_2 and ^6LiF down to 0.45 K and use this data to extrapolate the specific heats to 0.1 K.

2. Experimental

The TiB_2 sample was provided by Y-12 National Security Complex which had been originally obtained from Semi-Elements, Inc. of Saxonburg, PA (now defunct). From secondary ionization mass spectrometry (SIMS) and X-ray photoelectron spectroscopy (XPS), the sample was found to be 92% $TiB_{2\pm0.1}$ with 4% C and 4% O impurities. The sample measured was a single cylindrical specimen approximately 8 mm high and 5 mm in diameter and had an apparent metallic sheen. The sample weighed 0.5382 g, and was loaded on to the calorimeter by attaching it to the measurement platform using a small amount of Apiezon N grease. The total specific heat was measured from 0.47 to 100 K, then the specific heat of the TiB_2 was determined by subtracting the known specific heats of the empty calorimeter and Apiezon N grease from the total specific heat of the system.

The ^6LiF sample was formed from ^6LiF powder purchased from the Saint-Gobain Crystals and Detectors Company. The sample was assayed at 96% isotopic purity with a melting point of 848 °C. The powder was placed in a graphite liner and inserted into a fused silica ampoule. The sample was heated to 150 °C under dynamic vacuum of 4.4×10^{-7} Torr for 90 min to eliminate water present in the powder and the ampule was subsequently sealed. The sealed ampule with the ^6LiF powder was then placed in a Bridgeman furnace and lowered slowly from the hot zone (temperature just above the melting point) to the cold zone (temperature just below the melting point) to form a large single crystal. The crystal was cut to a square prism measuring 7 mm × 7 mm × 3.5 mm and was a clear, colorless single crystal with no visible internal defects. The sample weighed 0.4385 g and was also loaded onto the calorimeter platform with a small amount of Apiezon N grease. The specific heat of the calorimeter, Apiezon N grease, and the ^6LiF sample was then measured from 0.45 to 40 K. By subtracting the known specific heats of the calorimeter and Apiezon N grease from the total specific heat of the system, the specific heat of ^6LiF was determined.

The specific heats of both the TiB_2 and the ^6LiF were measured on an semi-adiabatic calorimeter built on a ^3He pumped cryogen stage that is immersed in liquid He. The working range of this instrument is typically from 0.45 K up to a maximum of 40–100 K, depending on the overall thermal conductivity of the sample. A description of a similar apparatus as well as additional details of the current apparatus can be found elsewhere [5,6]. The specific heat values obtained from this instrument typically have an accuracy better than 0.25% with a precision better than 0.1% based on measurements of a high purity copper sample. The TiB_2 and ^6LiF samples had a significantly smaller specific heat than copper, thus the results have an increased uncertainty. The approximate contributions to the total heat capacity for copper, TiB_2 and ^6LiF over various temperatures are given in Table 1 with an estimation of the overall uncertainty for the measured compounds.

The uncertainty calculations for our specific heat measurements is handled in a unique manner since the equilibrium adiabatic techniques that we use preclude us from performing repeat measurements at each temperature and, consequently, the use of standard statistical methods involving replicate measurements cannot be applied. Historically, estimates of the accuracy and precision (uncertainties) in specific heat data have been achieved by performing measurements on standard references materials such as copper or benzoic acid and comparing these results, including the precision of empirical and theoretical fits, to the results of other laboratories over a period of many decades. The uncertainty estimate for both TiB_2 and ^6LiF have been determined by the percent deviation from copper, as measured on this apparatus, and the ratio of the percent contribution of the respective sample heat capacity to the percent contribution of copper. The percent contribution is the fraction of the heat capacity attributed to the sample out of the total heat capacity (the heat

Table 1
Average percent contributions to the total specific heat and estimated uncertainty for copper, TiB_2, and LiF

T (K)	Percent contribution			Uncertainty (%)		
	Copper	TiB_2	^6LiF	Copper	TiB_2	^6LiF
0.5	73	49	4.6	0.2	0.3	3.5
1	73	47	7.9	0.22	0.32	2.0
5	57	15	7.4	0.22	0.72	1.5
10	55	6.9	9.3	0.22	0.84	1.1
20	65	4.1	14	0.21	1.3	0.89
30	70	4.3	19	0.21	1.5	0.67

capacity of the sample, the calorimeter, and Apiezon N grease). The error bars shown in all the figures are from this estimation of uncertainty which is summarized in Table 1; where there are no error bars, the uncertainty is less than the symbol size.

3. Results and discussion

The total molar specific heats of TiB_2 and ^6LiF are shown in Figs. 1 and 2, respectively. The measured specific heat of TiB_2 agrees fairly well with the previously published values of Westrum and Castaing, although the specific heat reported here is slightly lower [7,8]. This is likely due to the better crystallinity of the current sample and the higher stoichiometric ratio of boron in this sample than in earlier samples. (For example, the Westrum sample was characterized as $TiB_{1.96}$ and was a powdered sample rather than a single crystal [7].) The ^6LiF sample also has a lower measured specific heat when compared to previous measurements, but there is not as much difference here as was seen in the TiB_2 measurements. This is attributed to the enrichment of the ^6Li isotope, since lighter isotopes tend to give a lower specific heat. In this case, the previous measurements of both Clusius and Martin report the specific heats of LiF with natural isotopic abundance (7.52% ^6Li and 92.48% ^7Li), whereas in this sample, the lighter ^6Li isotope has been in-

creased from the natural abundance to 96% [9,10]. A simple isotopic correction can be applied to the specific heat using the square root of the ratio of the molecular weights, which results in good aggreement with the current data and the literature values, except below 5 K, where there is greater deviation from Martin's data, but Martin's data does fall within our experimental uncertainty. (It should be noted that the isotopic correction mentioned above only works well in the low-temperature limit, where the density of states can be modelled with an harmonic approximation.)

3.1. TiB_2

To extrapolate the specific heat of TiB_2 to 0.1 K, we must obtain a model of the lattice and electronic specific heats. Typically, at temperatures below 10 K, the lattice and electronic specific heat are determined using the Debye extrapolation, which when the data is plotted as C/T vs. T^2 (see Fig. 3) should be a linear fit of the equation $C/T = \gamma + \beta T^2$. For TiB_2, the trend is linear as expected, except below 2 K where the value of C/T begins a steep upturn. This upturn is attributed to the hyperfine splitting of nuclear moments of both Ti and B by local magnetic fields. Titanium has two naturally occurring isotopes with a nuclear spin and nuclear moment, ^{47}Ti and ^{49}Ti, but the
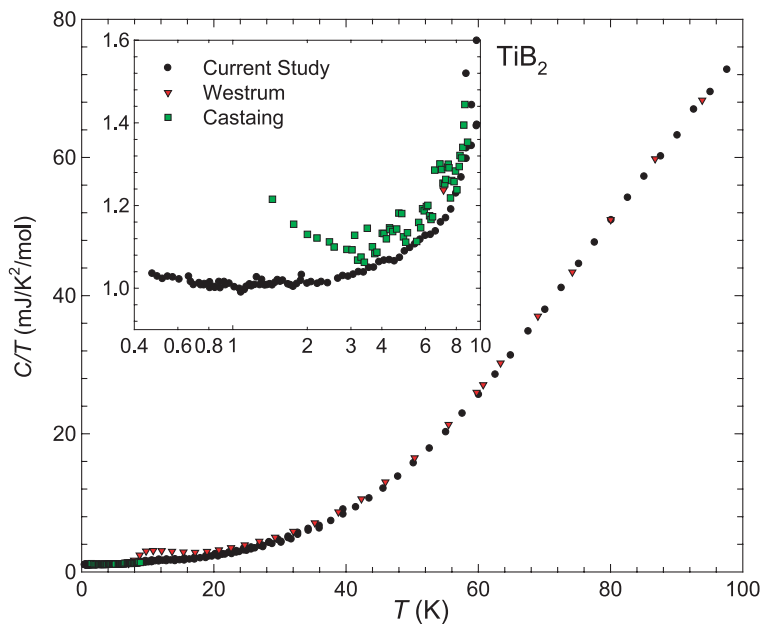

Fig. 1. Specific heat of TiB_2 from this study, along with the data from Westrum and Castaing from $T = 0.5$ to 100 K [7,8].
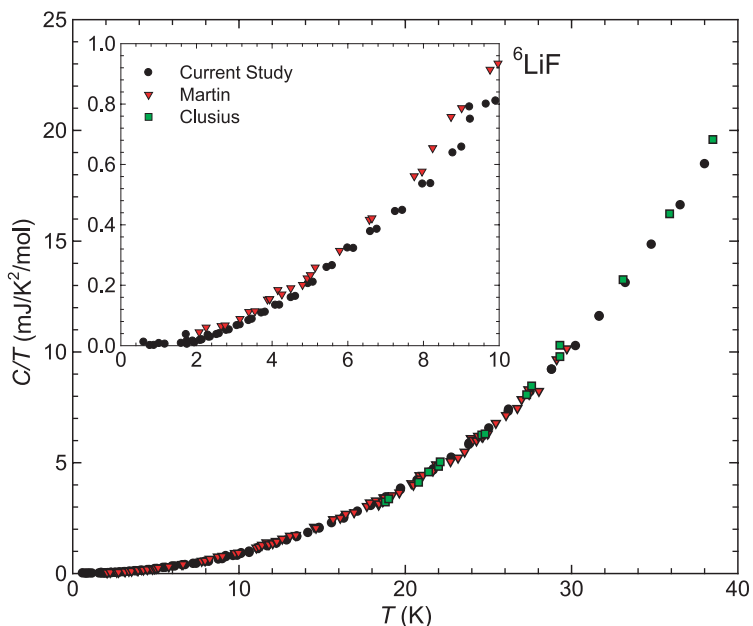
Fig. 2. Specific heat of LiF from this study, along with the data from Clusius and Martin from $T = 0.5$ to 40 K [9,10].
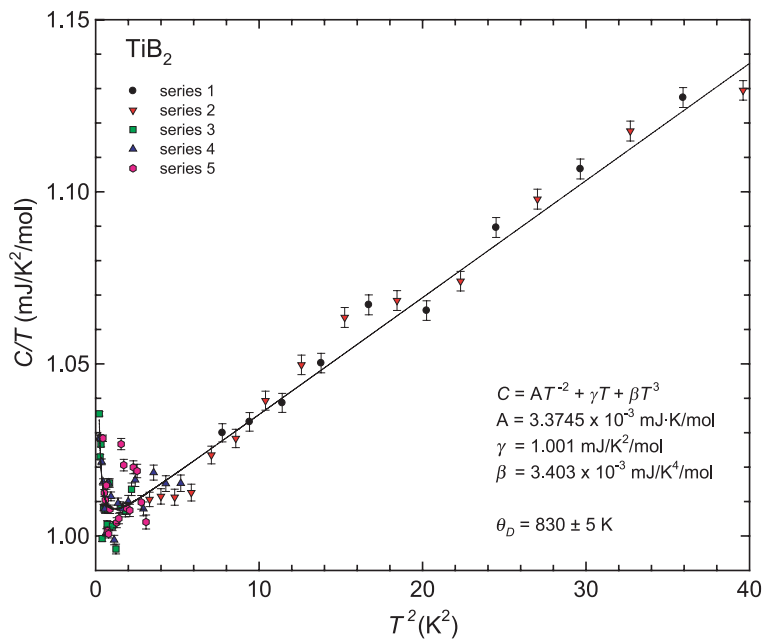

Fig. 3. Low-temperature Debye extrapolation of TiB_2 with the hyperfine contribution. The various symbols represent the different series of data collected.

combination of these are only 13.8% of the natural abundance and the nuclear moments of the isotopes are relatively small. Likewise, the isotopes of boron, ^{10}B and ^{11}B, also have nuclear spin and nuclear mo-

ments, but these isotopes constitute 100% of the natural abundance of boron. Furthermore, the nuclear moments of these isotopes are significantly larger than those of the titanium isotopes. Thus, the

contribution to the specific heat below 2 K is due almost entirely to the ordering of the nuclear spins of the boron isotopes.

In order to model the electronic and lattice specific heat at low temperatures, the specific heat was fit to an equation of the form:

$$C = AT^{-2} + \gamma T + \beta T^3, \qquad (5)$$

where AT^{-2} models the hyperfine contribution, γT is the electronic contribution, and βT^3 is the lattice specific heat. The resulting fit of this equation is shown in Fig. 3, and is plotted as C/T vs. T^2 to show that the specific heat has a linear component in the Debye extrapolation until the onset of the hyperfine contribution. Values of γ and β obtained from the fit are $1.001 \pm 0.019 \, \text{mJ/K}^2/\text{mol}$ and $3.403 \times 10^{-3} \pm 0.070 \times 10^{-3} \, \text{mJ/K}^4/\text{mol}$, respectively and are slightly lower than previously published results, which again is consistent with the nature of this sample [7,8]. (The uncertainty here is caluclated from the standard deviation of the slope and intercept.) Furthermore, the calculated Debye temperature, θ_D, for this sample is 830 ± 5 K compared to the values of 820 K and 807 from Castaing and Tyan, respectively, which is also consistent with using a sample that is higher in quality [8,11].

Although Eq. (5) adequately represents the experimental data to within experimental error, the AT^{-2} term is only an approximation of the high-temperature side of the hyperfine specific heat and cannot be used to predict the nuclear specific heat at low temperatures. To correctly extrapolate the specific heat to 0.1 K, a more exact model of the hyperfine contribution must be applied. Nuclear moments can generally be considered as two-level systems where the energies of the nuclear spin system populate one of the two levels. Specific heats of two-level systems are calculated from Schottky functions that have the form:

$$C_{\text{Schottky}} = nR\left(\frac{\theta_S}{T}\right)^2 \frac{g_0}{g_1} \frac{\exp(\theta_S/T)}{(1 + (g_0/g_1)\exp(\theta_S/T))^2}, \qquad (6)$$

where θ_S is the Schottky temperature, n is the number of level systems (moles) in the sample and g_0/g_1 is the ratio of the degeneracies of the two levels, which for the nuclear splitting is set to 1 [12]. The low-temperature specific heat can then be fit to the equation:

$$C_{\text{tot}} = C_{\text{Schottky}} + \gamma T + \beta T^3. \qquad (7)$$

Since we are only working with the high-temperature side of the Schottky function, two different models were used to predict the behavior of the spin system below our measurements. The first model assumes that there is a weak, local magnetic field present at every B atom throughout the sample. This implies that the hyperfine contribution arises from the splitting of the nuclear levels in each B atom and thus n in Eq. 6 must be set to 2, since there are 2 mol of boron per mole of TiB_2 assuming that boron gives the only contribution to the hyperfine splitting. The second model assumes that the magnetic moments are not uniform throughout the system, and would be consistent with the hyperfine contribution arising from bonding inhomogeneities in the system. This could result from interstitial vacancies in the Ti–B lattice or from impurities in the sample, changing the bonding characteristics in some fraction of the sample. This would imply that n in Eq. 6 represents the number of moles of the bonding inhomogeneities in the sample and should be allowed to float or vary in the fit and come to a 'best' value. In both models, the splitting of the two nuclear levels is represented by θ_S and is allowed to vary in the fit.

A summary of the fitting results for both hyperfine models is given in Table 2 and shown in Fig. 4. While both models yield similar results, the values of n and θ_S from the respective fits and what is known about the sample itself can give insight to the validity of the models. First, of the Schottky temperatures calculated from both models, the value of $\theta_S = 0.059$ K from the second model seems to be a more reasonable value based on comparisons to Schottky temperatures of similar boron compounds such as CaB_6 [13]. Although this is not a quantitative measure of the validity of the second model, it is a useful comparison since we expect there to be similar bonding in the two systems. Secondly, from the high degree of covalent bonding in the Ti–B system, it is not expected to have unpaired

Table 2
Summary of Schottky fits for TiB_2

	n	Θ_S (K)	C_p ($T = 0.1$ K) (mJ/K/mol)
Debye extrapolation	–	–	0.100 ± 0.001
Model 1	2	8.9×10^{-4}	0.435[a]
Model 2	4.5×10^{-4}	5.9×10^{-2}	0.408[a]

[a] Absolute uncertainties for the Schottky functions are unknown, but the maximum value for the uncertainties are estimated to be ± 0.027 mJ/K/mol.
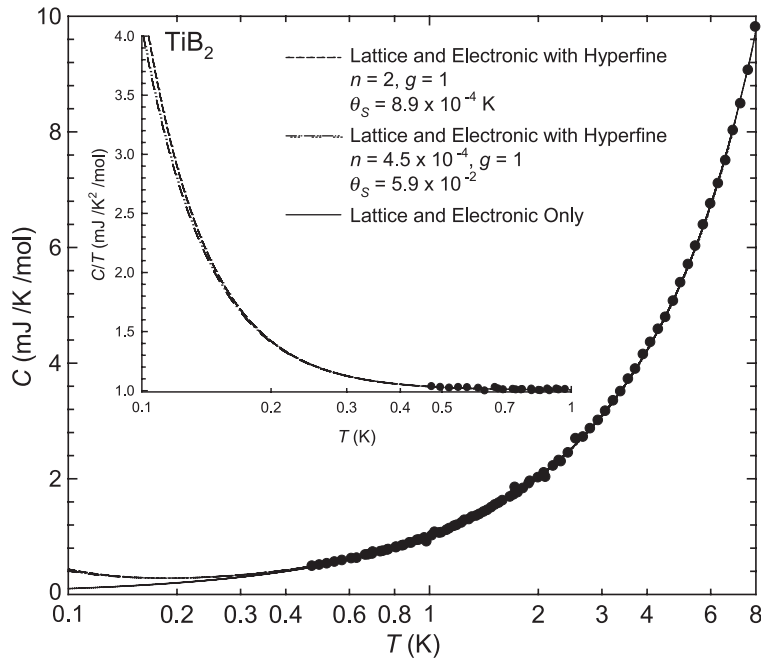
Fig. 4. Low-temperature fits of the lattice and electronic specific heats of TiB_2 along with the additional hyperfine models for the specific heats and the extrapolation of the specific heat to 0.1 K.

electrons that would contribute to the local magnetic field at each B atom. Also, previous measurements on poorer samples of TiB_2 show a larger upturn and a higher onset temperature, suggesting that this feature is sample dependent [8]. The first model assumes that the magnetic moment in the sample is homogeneous, and it implies that all Ti–B bonds are the same, and must, therefore, all have some ionic character. The second model attributes the magnetic moments of the sample to bonding inhomogeneities. The value of n from the second model, 4.5×10^{-4} mol, is more consistent with the defects and bonding inhomogeneities that would be expected from a crystalline sample.

Of the two calculated models and from what is known about the sample, the second model seems to be more plausible, although the first model cannot be completely ruled out. The second model gives a specific heat at 0.1 K of 0.408 ± 0.027 mJ/K/mol using the value at 0.1 K from the first model to estimate the uncertainty. The uncertainty in the extrapolated specific heat was estimated in this manner since (a) there are no statistical methods available for calculating the uncertainties in Schottky functions and (b) the first model is an upper bound for the number of spin states in the system and the difference in specific heat between the two models would

seem to provide a reasonable upper bound for the uncertainty. Presently, for a sample of this quality this would be the best calculation of the specific heat for TiB_2 at 0.1 K. It should be noted, however, that if the second model is correct, the size of the nuclear contribution (C_{Schottky}), and therefore, the value of the specific heat at 0.1 K, will be sample dependent since the concentration of bonding inhomogeneities will vary from sample to sample. Also implied with the second model is that the ideal or intrinsic specific heat will be one without the hyperfine splitting, and consequently, the extrapolation should only use the electronic and lattice terms in Eq. (5). Thus, the best case of intrinsic specific heat at 0.1 K would be $1.0 \times 10^{-4} \pm 0.01 \times 10^{-4}$ J/K/mol, although each sample of TiB_2 would have to be measured to obtain an accurate value for the specific heat.

3.2. LiF

As in the case of TiB_2, the Debye extrapolation was used for $T \leqslant 10$ to model the lattice and electronic specific heat of ^{6}LiF. Fig. 5 shows the plot of C/T vs. T^2; however, unlike TiB_2 there is no low-temperature upturn and the y-intercept is zero. The absence of the upturn in ^{6}LiF indicates there are no nuclear hyperfine interactions, and the

zero-intercept indicates the absence of an electronic contribution to the specific heat. In most respects, this makes the estimation of the low-temperature heat capacity easier since there is only the lattice contribution, but from Fig. 5 (and Table 1) it can

be seen that there is a greater uncertainty primarily due to the sample size and the significantly smaller heat capacity contribution.

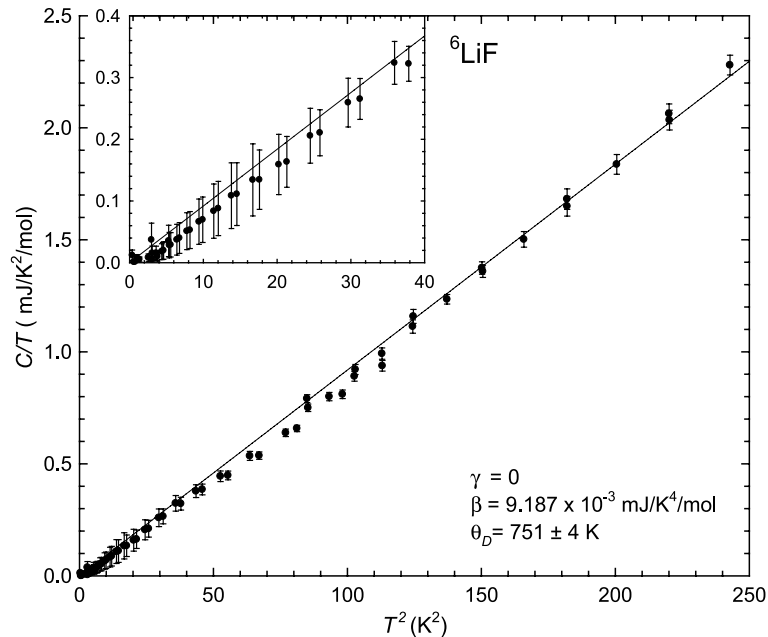Although ^{6}LiF has an increased uncertainty in the specific heat below 10 K, it was relatively easy

Fig. 5. Low-temperature Debye extrapolation of ^{6}LiF.

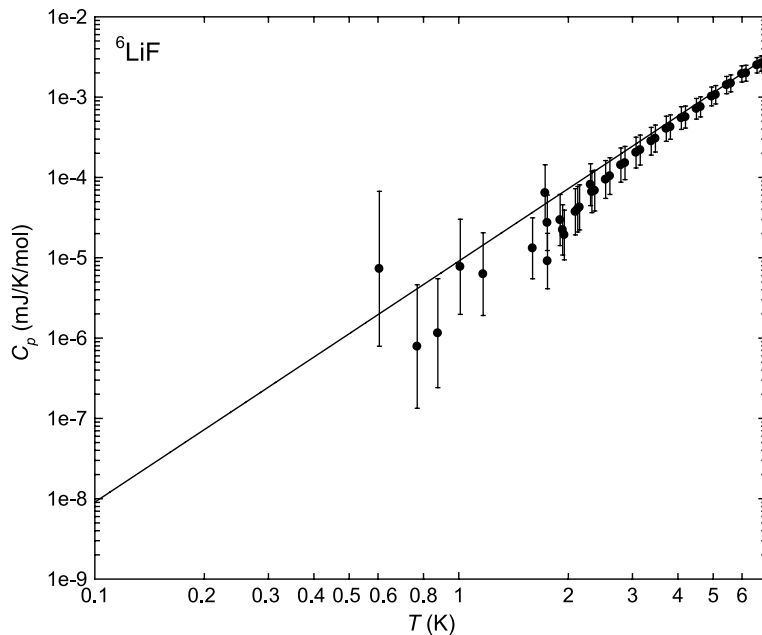Fig. 6. Low-temperature fits of the lattice specific heat of ^{6}LiF along with the of the specific heat down to 0.1 K.

to fit the data to an equation of the form $C = \beta T^3$ where the value of β was found to be 9.187×10^{-6} J/K^4/mol for $T^2 < 250$ K. This gives a Debye temperature of 751 ± 4 K, which is slightly higher than Martin's reported value of 737 ± 9 K [10]. This discrepancy can be attributed to the isotopic differences between the two samples. When an isotopic correction is applied, making an adjustment to the natural abundance of Li isotopes, the Debye temperature is 746 ± 4 K. Although this value is still slightly higher than that reported by Martin, it is within the error limits reported by Martin, thus this is an acceptable value for the Debye temperature.

The aim of these measurements was to calculate the heat capacity of ^{6}LiF at 0.1 K. Unlike the TiB$_2$ sample, the absence of any electronic and nuclear contribution makes the extrapolation down to 0.1 K relatively straightforward. It is only the uncertainty of the heat capacity values that causes complications in the calculations. However, extrapolating the lattice heat capacity of the ^{6}LiF to 0.1 K gives $C = 9.19 \times 10^{-9} \pm 0.15 \times 10^{-9}$ J/K/mol, where the uncertainty is obtained from the standard deviation of β. The resulting extrapolation of the specific heat to 0.1 K can be seen in Fig. 6.

4. Conclusion

This study has given us the best available values for the specific heats of TiB$_2$ and ^{6}LiF at 0.1 K. However, using the specific heat data of TiB$_2$ (especially extrapolated values) for thermodynamic purposes is not recommended since the specific heat appears to be highly sample dependent, which is further complicated by the complex nature of the Ti–B system. Indeed, if one examines the phase diagram for Ti–B there is a significant range of stoichiometric ratios that are considered TiB$_2$ [14]. From this and the variation in the specific heat between the current study and literature, it is likely that one must measure the low-temperature specific heat for

each sample of TiB$_2$ in order to obtain the most accurate value. ^{6}LiF, on the other hand, has a more consistent stoichiometric ratio, which should lead to more reproducible specific heat results. However, the specific heat is effected a great deal at low temperatures by the isotopic ratio of Li. Specifically, in this sample the enrichment of the ^{6}Li isotope from natural abundance to 96% gives a total molecular weight change of -3.4%; nonetheless, the isotopic specific heat difference can be easily accounted for in the low-temperature limit.

References

[1] G. Taubes, Bad Science: The Short Life and Weird Times of Cold Fusion, Random House, New York, 1993.
[2] D.T. Chow, M. Lindeman, M. Cunningham, M. Frank, T.W.J. Barbee, S.E. Labov, Nucl. Instrum. and Meth. A 444 (2000) 196.
[3] T. Niedermayr, I.D. Hau, T. Miyazaki, S. Terracol, A. Burger, V.A. Lamberti, Z.W. Bell, J.L. Vujic, S.E. Labov, S. Friedrich, Nucl. Instrum. and Meth. A 520 (2004) 70.
[4] S.H. Moseley, J.C. Mather, D. McCammon, J. Appl. Phys. 56 (5) (1984) 1257.
[5] J.C. Lashley, B.E. Lang, J. Boerio-Goates, B.F. Woodfeild, T.W. Darling, F. Chu, A. Migliori, D. Thoma, J. Chem. Thermodyn. 34 (2002) 251.
[6] B.F. Woodfield, Specific heat of high-temperature superconductors: Apparatus and measurement, PhD thesis, University of California, Berkeley, 1995.
[7] E.F.J. Westrum, G.A. Clay, J. Chem. Thermodyn. 10 (1978) 629.
[8] J. Castaing, R. Caudron, G. Toupance, P. Costa, Solid State Commun. 7 (1969) 1453.
[9] K. Clusius, J. Goldman, A.Z. Perlick, Zaturforschg 4a (1949) 424.
[10] D.L. Martin, Philos. Mag. 46 (1955) 751.
[11] Y.S. Tyan, L.E. Toth, Y.A. Chang, J. Phys. Chem. Solids 30 (1969) 785.
[12] E.S.R. Gopal, Specific Heats at Low Temperatures, Plenum Press, New York, 1966.
[13] P. Vonlanthen, E. Felder, L. Degiorgi, H. Ott, D. Young, A. Bianchi, Z. Fisk, Phys. Rev. B 62 (2000) 10076.
[14] X. Ma, C. Li, Z. Du, W. Zhang, J. Alloys Compd. 370 (2004) 149.